Hindawi
Disease Markers
Volume 2022, Article ID 6703053, 18 pages
https://doi.org/10.1155/2022/6703053

Research Article

Identification of Prognostic Genes and Immune Landscape Signatures Based on Tumor Microenvironment in Lung Adenocarcinoma

Pengkai Han,[1] **Yunxiu Fan**,[2] **Qiping Liu**,[1] **and Junhao Zhou**[1]

[1]*Department of Pulmonary and Critical Care Medicine, Chongqing University Three Gorges Hospital, Chongqing 404100, China*
[2]*Department of Oncology, Chongqing University Three Gorges Hospital, Chongqing 404100, China*

Correspondence should be addressed to Qiping Liu; liuqp1113@163.com and Junhao Zhou; 540808919@qq.com

Received 21 April 2022; Revised 14 June 2022; Accepted 29 July 2022; Published 18 August 2022

Academic Editor: Yuanwei Zhang

Background. Lung adenocarcinoma is the most common lung cancer subtype and accounts for the highest proportion of cancer-related deaths. The tumor microenvironment influences prognostic outcomes in lung adenocarcinoma (LUAD). *Materials and Methods*. We used the ESTIMATE algorithm (Estimation of STromal and Immune cells in MAlignant Tumor tissues using Expression data) to investigate the role of microenvironment-related genes and stromal cells in lung adenocarcinoma prognosis. This analysis was done on lung adenocarcinoma cases from The Cancer Genome Atlas (TCGA). The cases were divided into high and low groups on the basis of immune and stromal scores, respectively. *Results*. There were close correlations between immune scores with prognosis and disease stage. There were 367 differentially expressed genes. Combining the Gene Expression Omnibus (GEO) database, we found 14 prognosis-related genes. *Results*. Based on the enrichment levels of the immune cell types, we clustered LUAD into Immunity_H and Immunity_L subtypes. Most of these genes were upregulated in Immunity_H subtype. Finally, using the Human Protein Atlas (HPA) and the Clinical Proteomic Tumor Analysis Consortium (CPTAC) databases, most of the proteins corresponding to prognostic genes were verified to be differentially expressed between the tumor and normal groups. *Conclusions*. The key genes identified in this study are involved in molecular mechanisms of LUAD.

1. Introduction

Globally, lung cancer is the most common tumor type and the leading cause of tumor-related deaths. Non-small-cell lung cancer (NSCLC) accounts for more than 80% of all lung cancer cases. Lung adenocarcinoma (LUAD) is a common class of NSCLC [1]. LUAD constitutes half of all lung cancers and is associated with high morbidity rates.

Despite advances in screening, diagnosis, and lung cancer management, clinical outcomes remain poor. Lung tumors with different genetic and biological features may have different prognoses and drug responses. Genomic and biological features have been considered for prediction of cancer risks [2, 3]. However, tumorigenesis is driven by multiple factors and mechanisms. Tumor tissues comprise the parenchyma and interstitium. Tumor cells make up the parenchyma and are the main components of the tumor while the interstitium, which is composed of connective tissues, blood vessels, and immune cells and provides support and nourishment. Coevolution of tumor cells and the tumor microenvironment (TME) provides the basis for cancer cell proliferation and metastasis. Tumor cells have a remarkable ability for infinite proliferation, escape from the immune system, local invasion, and distant metastasis. Various factors in the TME promote cancer progression [4]. Stromal cells influence tumorigenesis and cancer progression [5] and drug fast [6]. Tumor cells and recruited immune cells in the tumor microenvironment contribute to cancer outcomes [7]. As such, assessing TME functions has been proposed as a diagnostic strategy [8]. Currently, the role of the TME, which is composed of immune and stromal cells, in cancer progression is vaguely understood. In LUAD, it has not been fully established how tumor biomechanisms and TME variations affect patient outcomes.

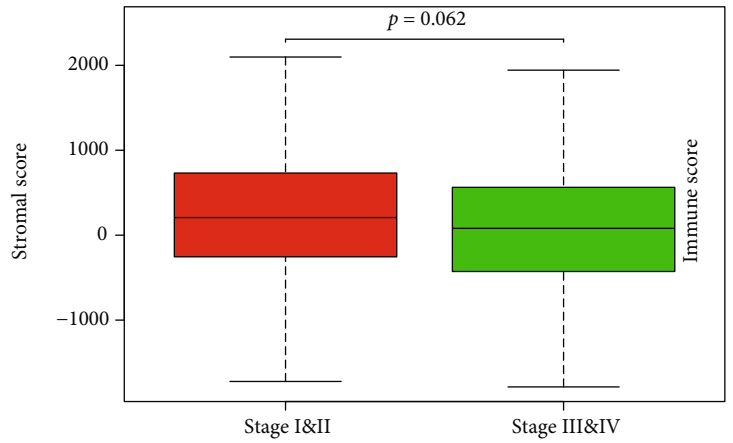

(a)

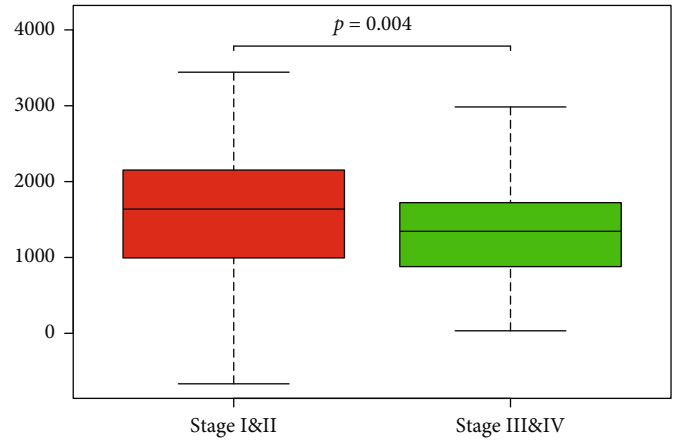

(b)

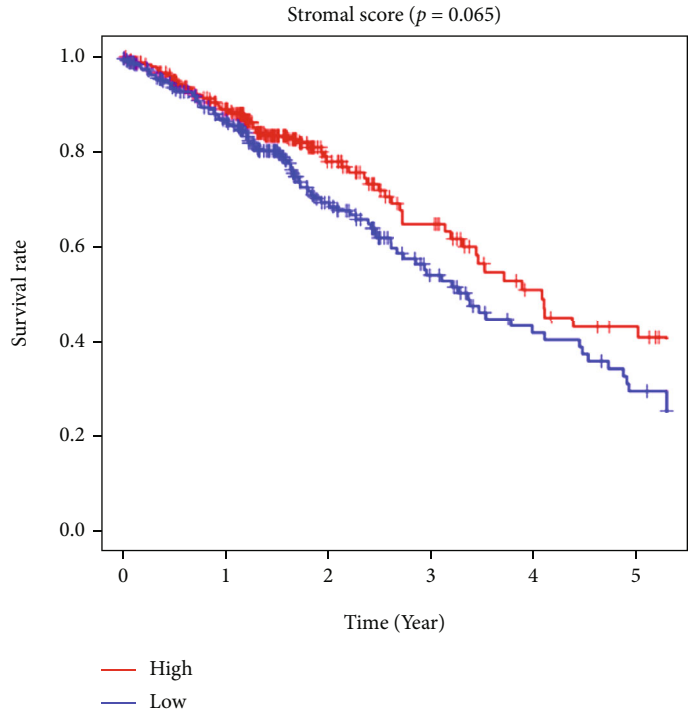

(c)

Figure 1: Continued.

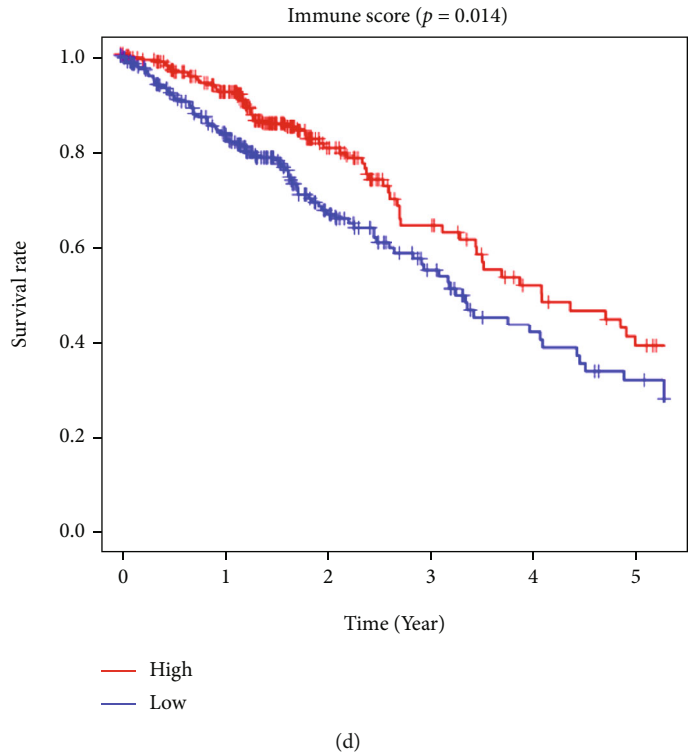

(d)

Figure 1: ESTIMATE scores in clinical stages and survival curves. (a) Comparison of stromal scores across clinical stages. (b) Comparison of immune scores across clinical stages. (c) Survival curve of stromal scores. (d) Survival curve of immune scores. ESTIMATE: Estimation of STromal and Immune cells in MAlignant Tumor tissues using Expression data.

Innate tumor genes determine tumor occurrence and development. The TME influences gene expressions and cancer outcomes [9, 10]. The TME can be evaluated by methods based on mRNA expression data. The ESTIMATE (Estimation of STromal and Immune cells in MAlignant Tumor tissues using Expression data) algorithm was used to assess immune and stromal cell infiltrations [10]. Gene expression and clinical data were obtained from The Cancer Genome Atlas (TCGA) and Gene Expression Omnibus (GEO) database [11].

Using LUAD gene expression data from TCGA, ESTIMATE was applied to evaluate the infiltrations of cells constituting the TME and screened a series of TME-associated genes. Further, survival analysis of these genes was performed using TCGA and GEO databases. Finally, corresponding protein expressions of each prognostic gene were validated.

2. Materials and Methods

2.1. Data Acquisition and Screening. Patient information for LUAD gene expressions as of May 2020 was downloaded from TCGA database [11] (https://portal.gdc.cancer.gov/). We analyzed 594 samples, of which 59 were normal lung tissues while 535 were tumor tissues. Clinical data included gender, age, and prognosis. Gene IDs were annotated in the gene transfer format. For validation analysis, gene expression data for LUAD patients were downloaded from the GEO database (GSE3141, GSE30219, and GSE31210 datasets) (http://www.ncbi.nlm.nih.gov/geo) along with disease outcome data. The above cases with expression data were included in the study. For survival analysis, only cases with survival information were selected.

2.2. Evaluation of Immune Cells and Acquisition of ESTIMATE Scores. The ssGSEA procedure was used to obtain enrichment scores for each specific term. Marker genes for 29 immune cell subtypes were obtained from published literature (Table S1). The ESTIMATE score system consists of the immune and stromal scores [12]. ESTIMATE analyzes bulk tumor data and predicts tumor purity and immune as well as stromal cell infiltrations by single-sample gene set expression analysis (ssGSEA) [10]. Immune and stromal scores denote immune and stromal cell infiltrations, respectively. ESTIMATE analysis was performed using "ESTIMATE" in R (https://bioinformatics.mdanderson.org/estimate/rpackage.html). Patients were assigned into different groups depending on ESTIMATE scores. Survival time for patients in different groups was compared by survival analysis. Differences in ESTIMATE scores among clinical stages were also investigated.

2.3. Identification of Differentially Expressed Genes (DEGs). The limma R package [13] for analysis of high-throughput genomic data was used to analyze the corresponding dataset. With the mean of immune and stromal scores as the boundary values, all cancer cases were assigned into low and high groups. The original P values were adjusted. False discovery rate (FDR) and fold changes (FC) were calculated

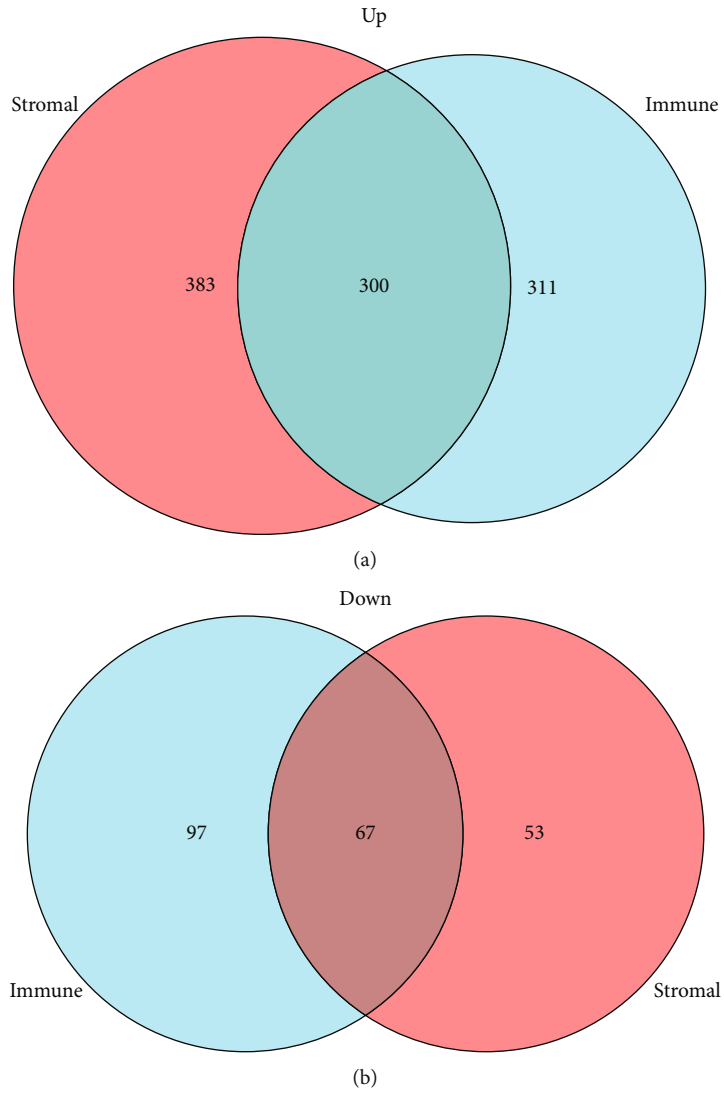

Figure 2: Venn diagram of DEGs based on immune and stromal scores. (a) Venn diagram showing upregulated DEGs. (b) Venn diagram showing downregulated DEGs. DEGs: differentially expressed genes.

to identify DEGs. The intersection of DEGs obtained by immune score and matrix scores was determined by Venn diagram analysis.

2.4. GO and KEGG Enrichment Analysis. GO term analysis was performed to elucidate on the biological processes (BP), cellular components (CC), and molecular functions (MF) in which the genes were enriched. GO and KEGG enrichment analyses were performed using clusterProfiler and DOSE packages in R [14]. $P < 0.05$ indicated significantly enriched pathways.

2.5. Overall Survival Analysis of DEGs. The relationship between survival time and gene expression levels of DEGs was determined by the log-rank test. Kaplan-Meier curves were plotted to visualize the relationships.

2.6. Clustering Analysis. Based on enrichment levels (ssGSEA scores) of the 29 immune cells, hierarchical clustering of LUAD was performed to identify different patterns of immune cell infiltrations and divided the LUAD cases into Immunity_H and Immunity_L subtypes. Then, differences in ESTIMATE scores and prognostic gene expressions between the immune subtypes were compared.

2.7. Assessment of Prognostic Gene Expressions at the Protein Level. Protein expressions of prognostic genes were validated using the Clinical Proteomic Tumor Analysis Consortium (CPTAC, https://proteomics.cancer.gov/programs/cptac) and the Human Protein Atlas databases (HPA, https://www.proteinatlas.org). Immunohistochemical and proteomic results were explored to verify their differential expressions in tumor and normal tissues. This study was conducted according to the flow chart shown in Figure S1.

2.8. Statistical Analysis. The R software (version 3.5.3; https://www.r-project.org/) was used for statistical analysis and to visualize the results. ESTIMATE package was used to run ESTIMATE analysis. Through the GSVA package in R software, ssGSEA was used to quantify the infiltration

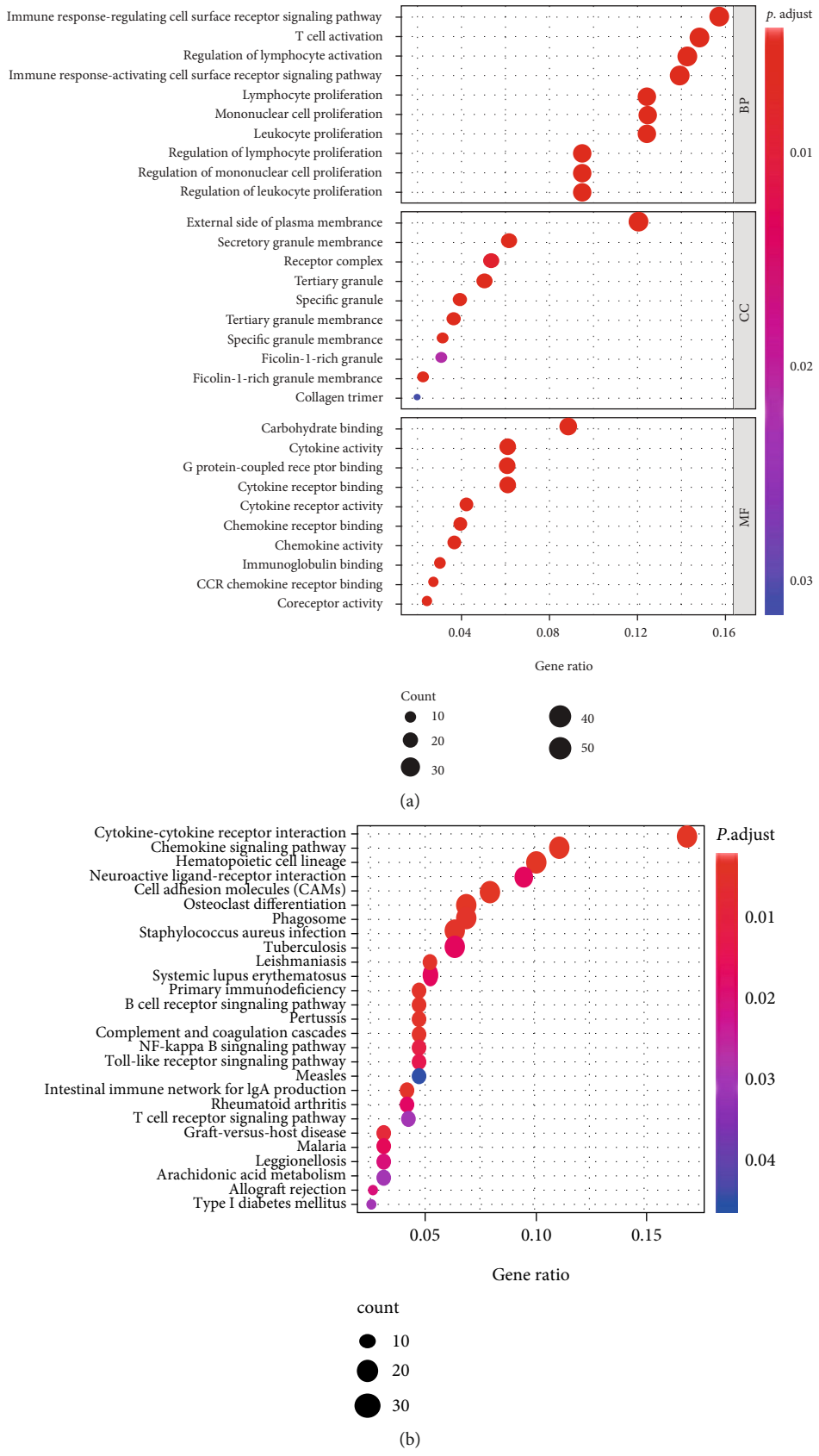

Figure 3: GO and KEGG pathway analysis for DEGs based on TME scoring model. (a) GO term enrichment; top ten pathways of each category with $P < 0.05$ are shown. (b) KEGG pathway enrichment. Top thirty pathways with $P < 0.05$ are shown. GO: Gene Ontology; KEGG: Kyoto Encyclopedia of Genes and Genomes.

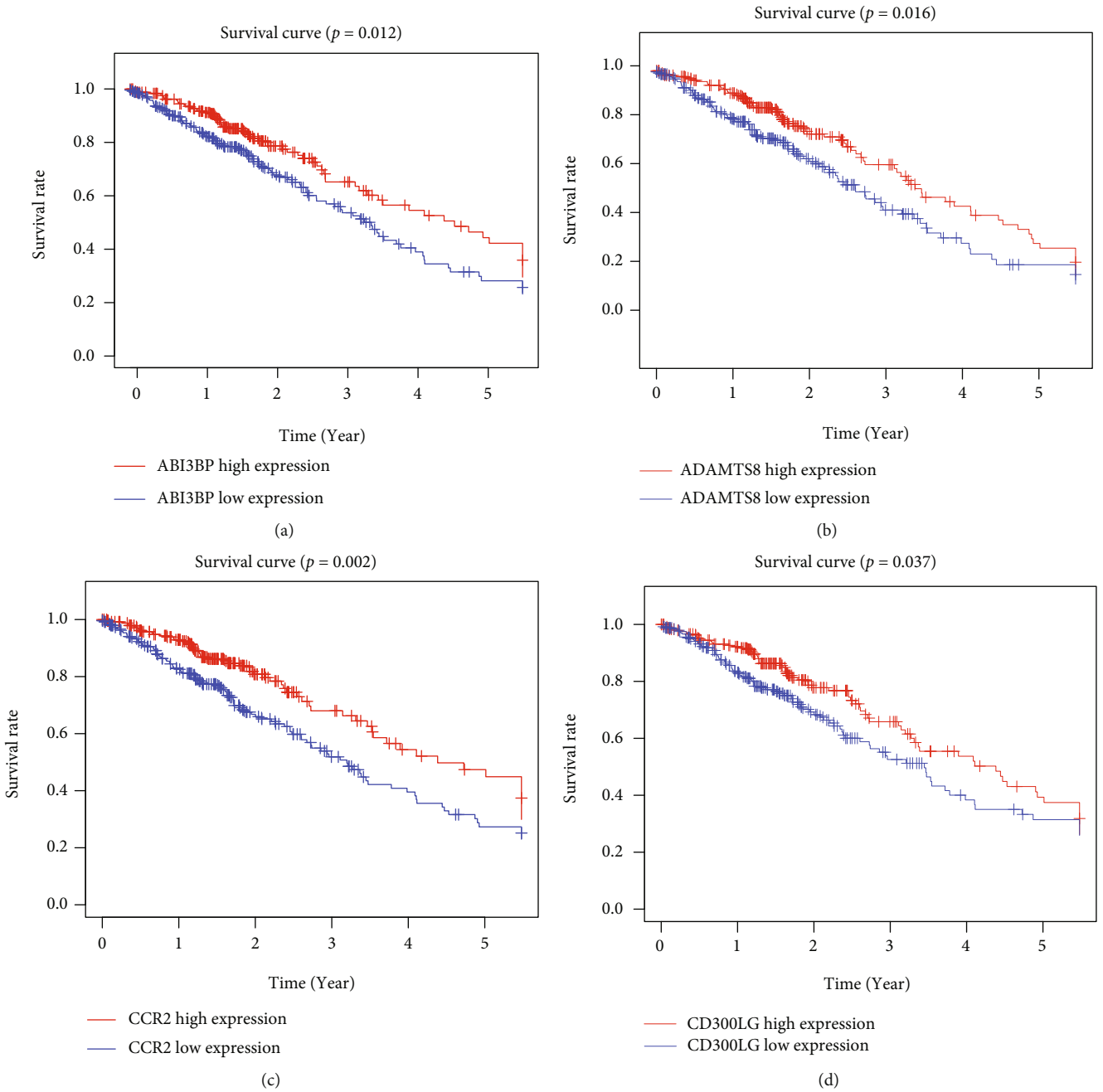

Figure 4: Continued.

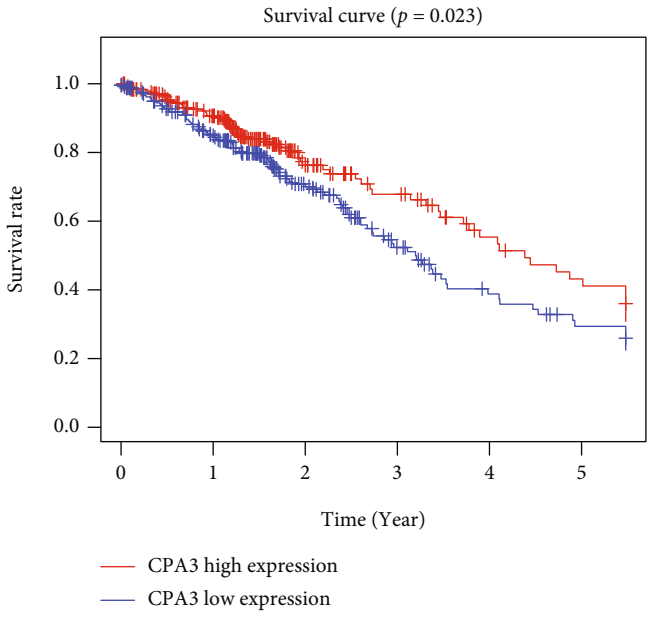

(e)

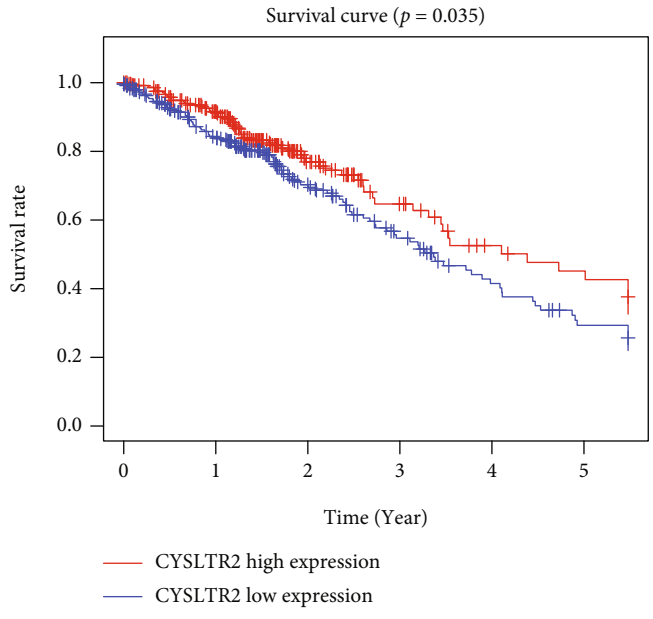

(f)

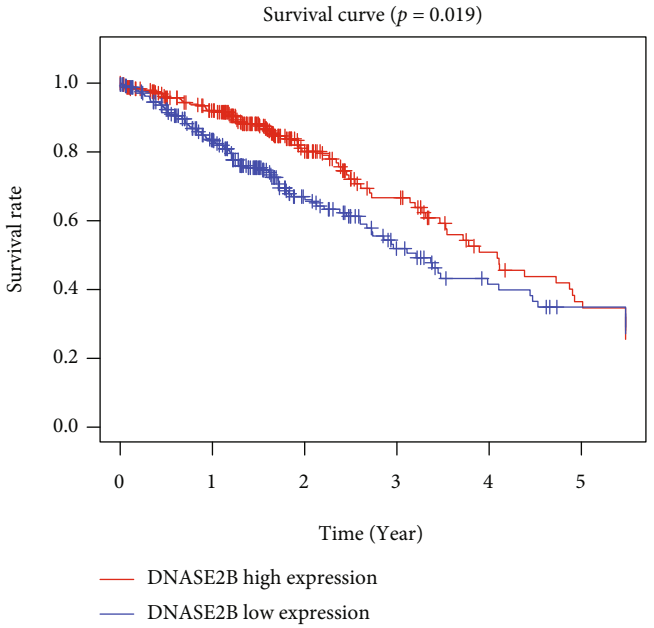

(g)

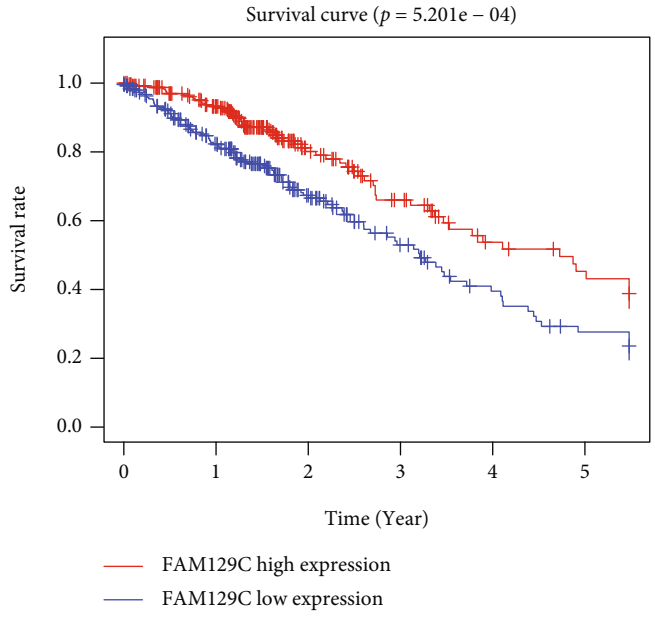

(h)

Figure 4: Continued.

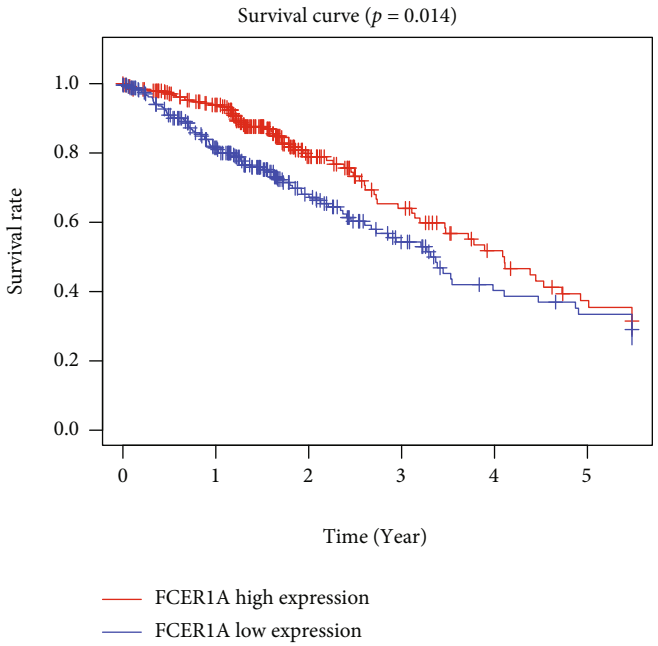

(i)

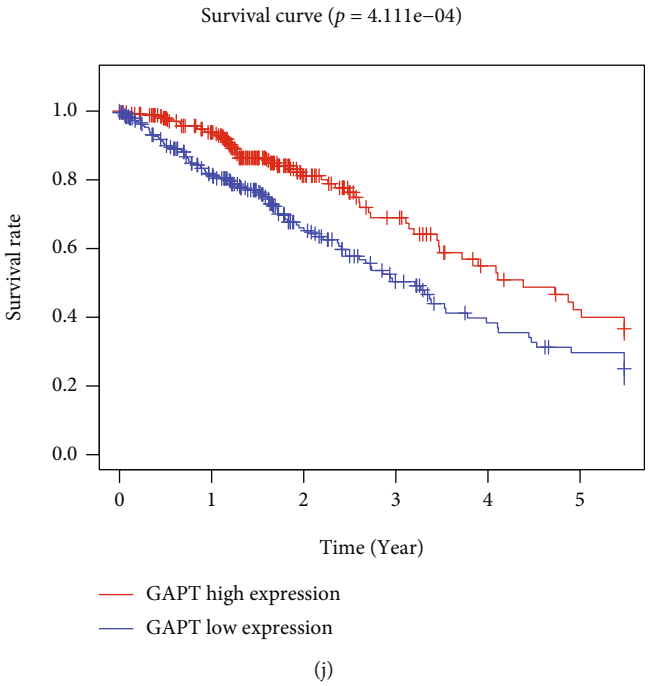

(j)

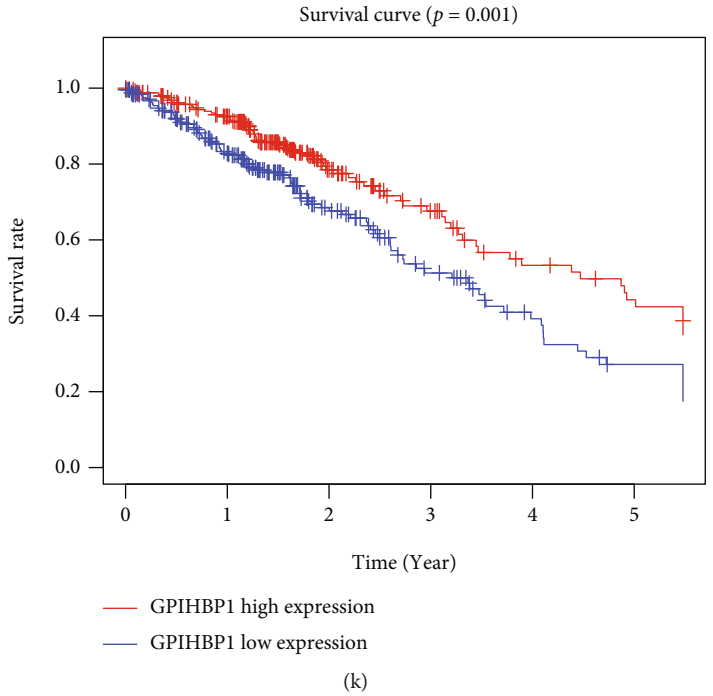

(k)

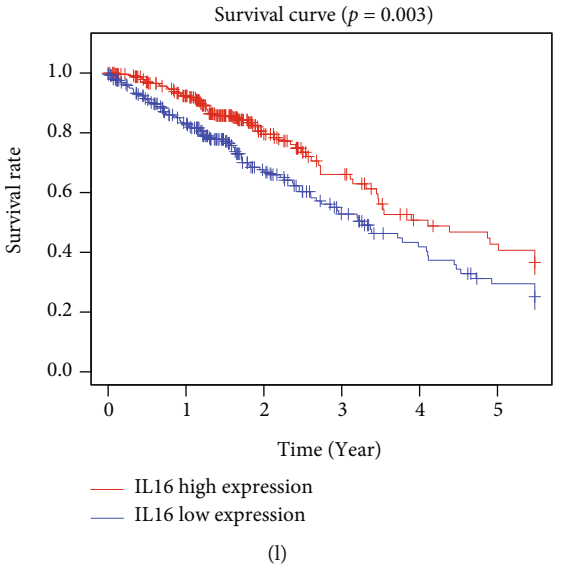

(l)

Figure 4: Continued.

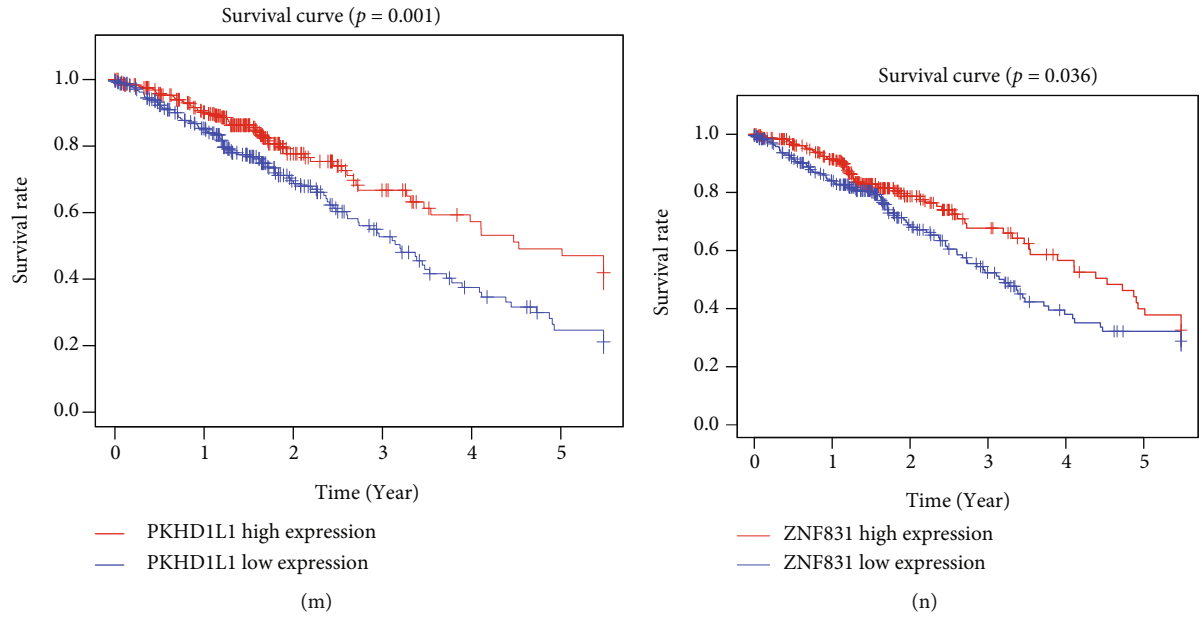

Figure 4: Prognostic value of mRNA expression (Kaplan-Meier plotter) of DEGs based on TME scoring model in LUAD patients. (a–n) Show the relation of mRNA expression of DEGs with the prognosis in LUAD patients from TCGA cohort using Kaplan-Meier plotter. Kaplan-Meier survival curves were generated for selected DEGs from high (red line) and low (blue line) gene expression groups. DEGs: differentially expressed genes; TME: tumor microenvironment.

levels of immune cell types (http://www.bioconductor.org/packages/release/bioc/html/GSVA.html). The limma R package was used to identify DEGs. DEGs were identified by comparing gene expressions between low and high score groups using the criteria: mRNA expression values of $|\log 2\,FC| > 1$ and $FDR < 0.05$. GO and KEGG enrichment analyses were performed using clusterProfiler and DOSE packages. Hierarchical clustering of LUAD was performed using the sparcl package. Survival analyses were performed using Kaplan-Meier survival analysis while log-rank tests were performed using survival R package. Comparisons of prognostic gene expressions between groups were performed by the T test. $P \leq 0.05$ was the threshold for statistical significance.

3. Results

3.1. Immune Scores Were Significantly Associated with LUAD Clinical Stages. Data on a cohort of 522 LUAD cases with mRNA expression profiles and corresponding clinical data were downloaded from TCGA. Of these, 280 cases were female while 242 male. In this analysis, immune scores ranged from -942.51 to 3442.08 while stromal scores ranged from -1789.62 to 2097.96. In various LUAD stages, immune scores were significantly high in stages I and II, relative to stages III and IV, indicating higher TME immune infiltrations in stages I and II (Figure 1(b)). There were no significant differences in stromal scores among different stages (Figure 1(a)). Clinical characteristics for all cases in this study are shown in Table S2.

3.2. Immune Score as a Potential Prognostic Marker for LUAD. To determine the effects of ESTIMATE scores on overall survival, cases were assigned into high and low score groups based on median ESTIMATE scores. Differences in survival time between high and low ESTIMATE score groups are presented using survival curves. Immune score analysis revealed a high survival rate, relative to the high score within five years ($P = 0.019$ in log-rank test, Figure 1(d)). A similar trend was observed for stromal scores, although the differences were insignificant ($P = 0.099$) (Figure 1(c)).

3.3. Differentially Expressed Genes with Immune and Stromal Score Groups in LUAD. Venn diagram analysis was used to identify co-DEGs in immune and stromal categories (Figure 2). There were 300 simultaneous upregulated genes in high score groups based on immune and stromal scores and 67 downregulated genes.

3.4. GO and KEGG Enrichment Analysis. To explore the functions of DEGs in LUAD, GO term and KEGG analyses were performed using R packages. Significantly enriched GO terms for DEGs were in BPs of immune responses regulating signaling pathways, lymphocyte proliferation, and mononuclear cell proliferation. Enriched MF processes included carbohydrate binding, immunoglobulin binding, and chemokine activity. Enriched CCs included external side of the plasma membrane, tertiary granule membrane, and tertiary granule (Figure 3(a)). Go term analysis revealed that the DEGs were predominantly correlated with immune functions. These findings are in agreement with previous reports that immune cells and the extracellular matrix are involved in lung TME [15]. KEGG pathway analysis indicated that DEGs were mainly enriched in cytokine-cytokine receptor interactions, hematopoietic cell lineage, and chemokine signaling pathway (Figure 3(b)).

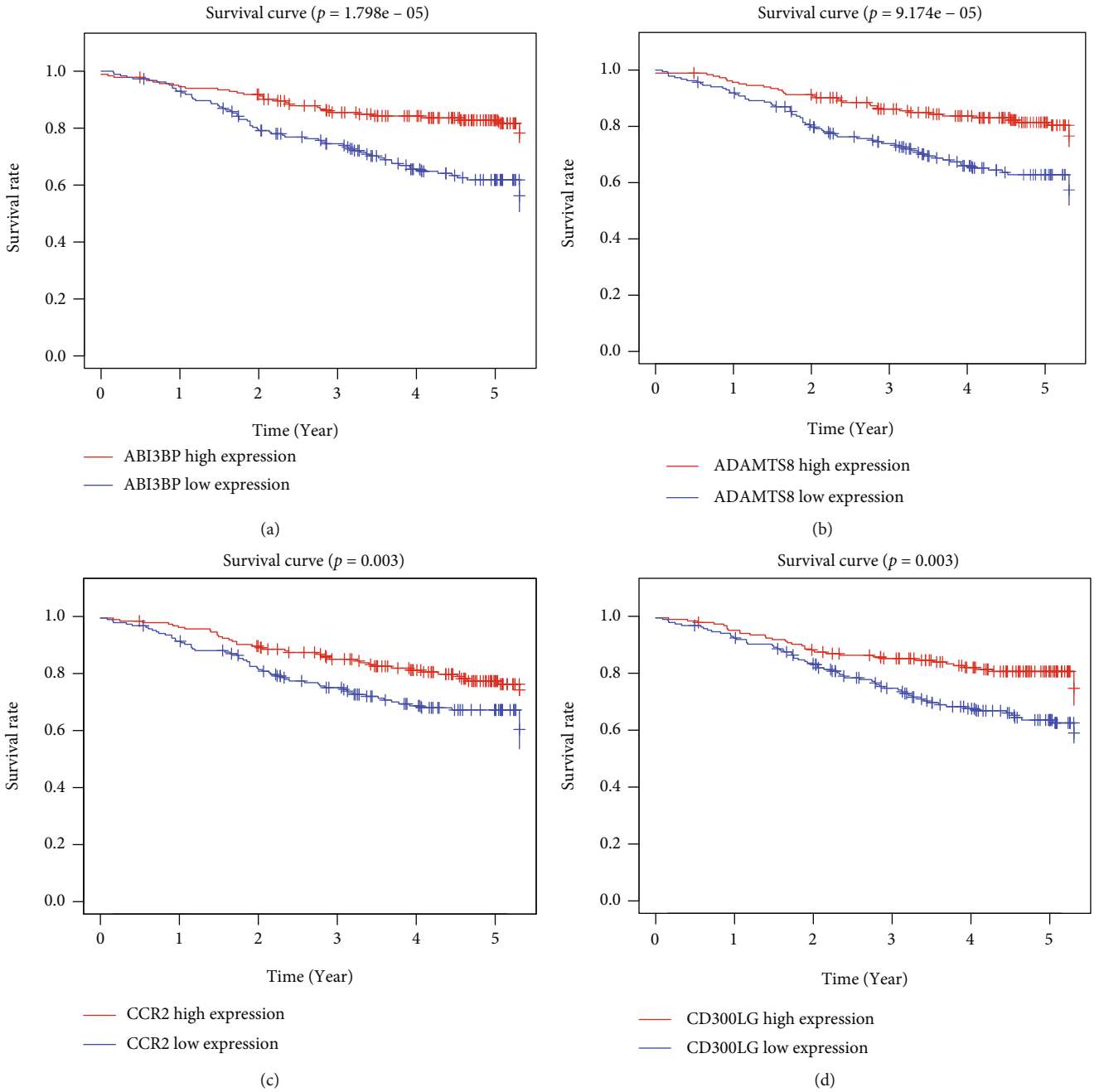

Figure 5: Continued.

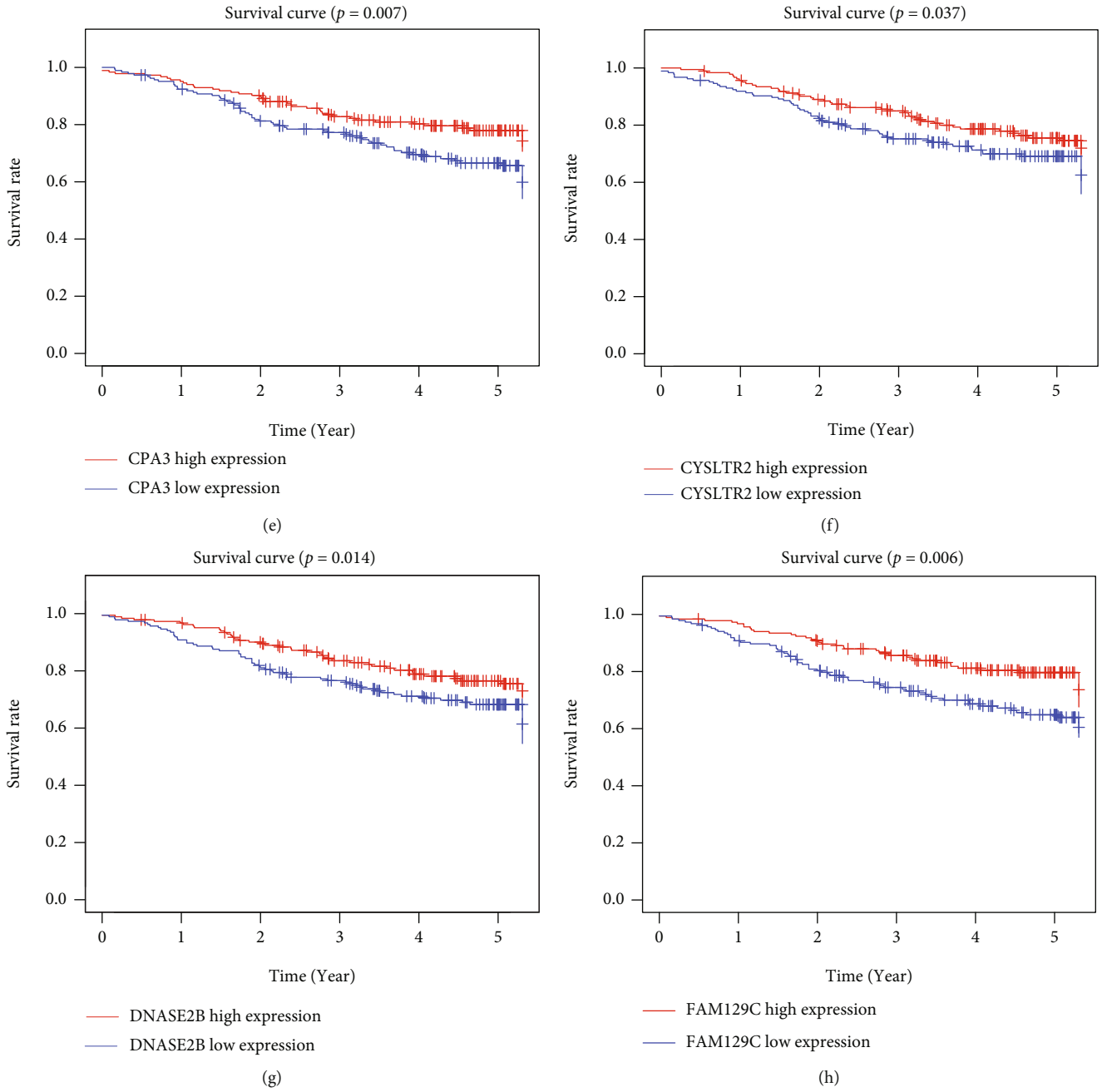

Figure 5: Continued.

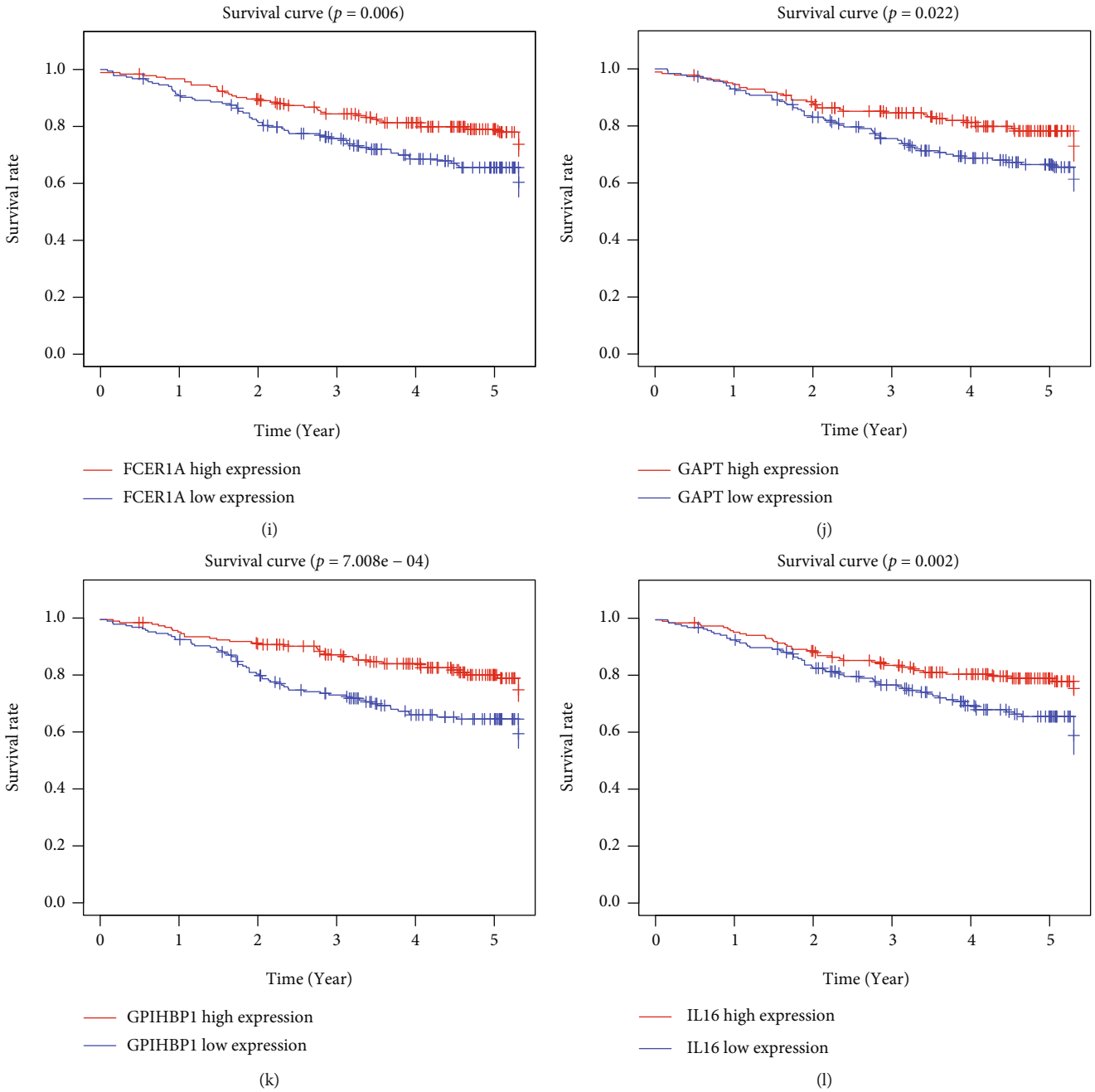

Figure 5: Continued.

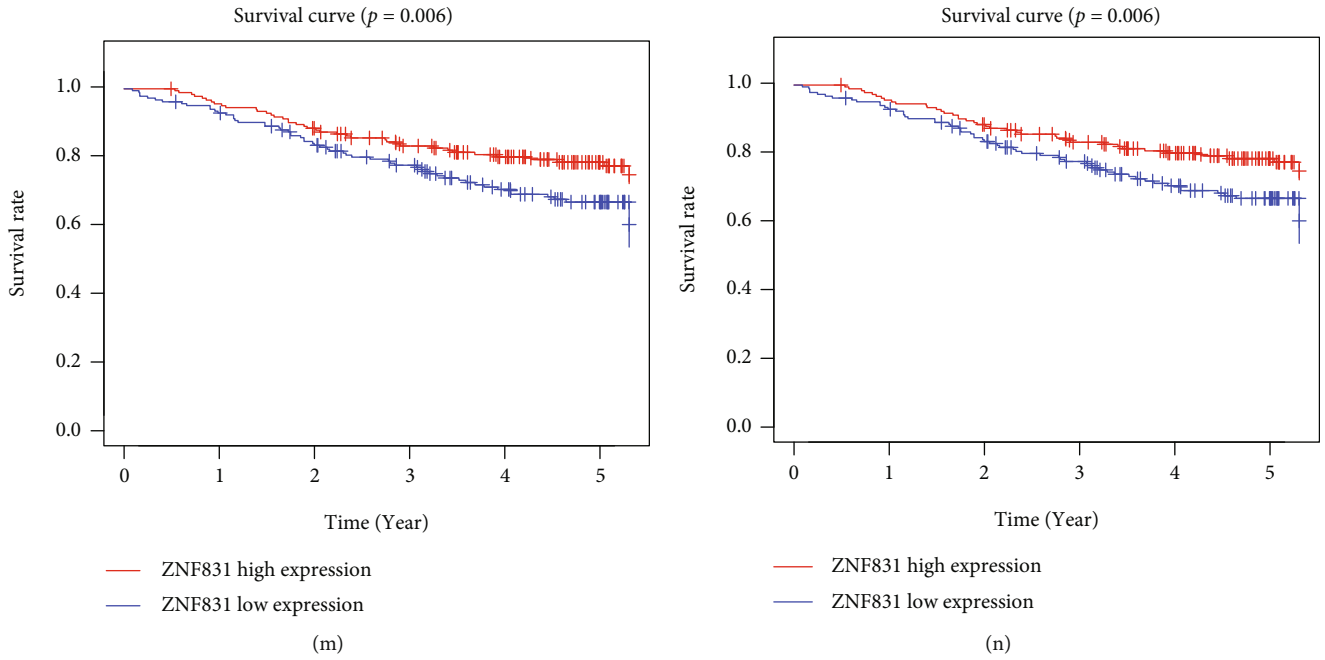

Figure 5: Prognostic value of mRNA expression (Kaplan-Meier plotter) of DEGs based on TME scoring model in LUAD patients. (a–n) Show the relation of mRNA expression of DEGs with the prognosis in LUAD patients from GEO cohort using Kaplan-Meier plotter. Kaplan-Meier survival curves were generated for selected DEGs from high (red line) and low (blue line) gene expression groups. DEGs: differentially expressed genes; TME: tumor microenvironment; DEGs: differentially expressed genes.

3.5. Survival Analysis with Gene Expressions of DEGs. To elucidate on the effects of DEGs on overall survival outcomes of LUAD patients, TCGA database was used to generate Kaplan-Meier survival curves. $P \leq 0.05$ indicated significant differences in survival outcomes. Among the 367 DEGs, 119 were significantly correlated with survival time, as revealed by log-rank test (Table S3). To validate the observations made in TCGA LUAD cohort in a different cohort, we analyzed the gene expression data for 369 LUAD cases in GEO. It was validated that 66 genes were significantly associated with LUAD prognosis (Table S4), while 14 genes were at the intersection of TCGA and GEO databases, which have relationships with survival (Figures 4 and 5).

3.6. Immune Landscape of Immune Clusters. Based on ESTIMATE and ssGSEA, immune characteristics of immune subtypes were visualized in the heat map (Figure 6(a)). Immune and stromal scores were significantly high in Immunity_H subtype and low in Immunity_L subtype. This indicated that the finding from ESTIMATE analysis was consistent with ssGSEA. Furthermore, expressions of the 14 prognosis-associated genes were compared in different immune subtypes. Expressions of most of these genes significantly increased from Immunity_L subtype to Immunity_H subtype (all $P < 0.001$; Figure 6(b)).

3.7. Differential Expressions of Prognostic Genes at the Protein Level. In the CPTAC database, ABI3BP, IL16, and CPA3 were found to be significantly downregulated in LUAD samples (Figure 6(c)). In the HPA database, protein expressions of the seven genes (ADAMTS8, CCR2, CYSLTR2, FAM129C, FCER1A, GAPT, PKHD1L1, and ZNF831) were markedly low in tumor tissues with less intense antibody staining and fewer stained cells in LUAD (Figure 7). GPIHBP1, CD300LG, and DNASE2B were not shown in either CPTAC or HPA databases.

4. Discussion

In this study, we identified 14 tumor microenvironment-related prognostic genes in lung adenocarcinoma from TCGA and GEO databases. Based on enrichment levels of immune cell types, we clustered LUAD into Immunity_H and Immunity_L subtypes. These genes were upregulated in Immunity_H subtype, indicating that they were closely associated with immune cell infiltrations in LUAD.

LUAD is often diagnosed in advanced stages. It is characterized by high metastasis and poor prognosis. Despite advances in LUAD treatment, long-term prognosis remains poor. In recent years, efforts have been made to identify potential prognostic markers for LUAD. For instance, the prognostic potential of LUAD gene expression signatures has been extensively studied [16].

Currently, TNM staging is the main basis for determining lung cancer prognosis. However, its effectiveness is limited by the fact that clinical outcomes for different patients at the same TNM stage can vary significantly [17]. Disease progression is influenced by immune cell infiltrations in the TME. In several cancers, immune-related indicators correlate better with clinical outcomes, relative to TNM staging [18–20]. Therefore, immune scores associated with TME are essential components of the staging system [21]. Development of immune checkpoint inhibitors, including

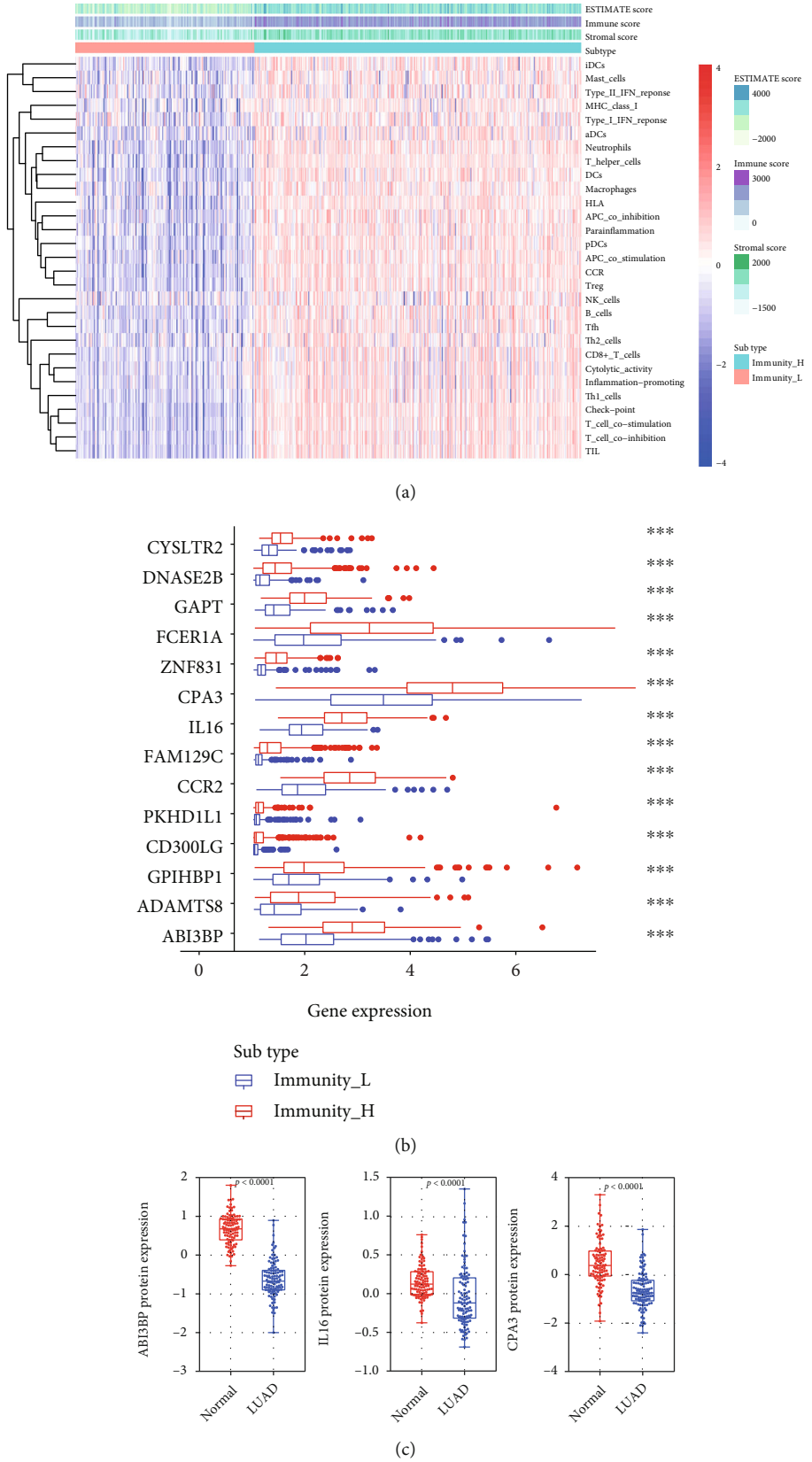

Figure 6: Immune landscape of immune subtypes. (a) Stromal score and immune score in different immune subtypes. The red and blue colours used on the heat map indicate the high and low relative activity of immune cells, respectively. (b) Comparison of prognostic gene expression levels between immune subtypes. $^{*}P < 0.05$, $^{**}P < 0.01$, and $^{***}P < 0.001$. (c) Comparisons of the expression at protein level of the three genes between lung adenocarcinoma (LUAD) and normal tissues in CPTAC. CPTAC: the Clinical Proteomic Tumor Analysis Consortium.

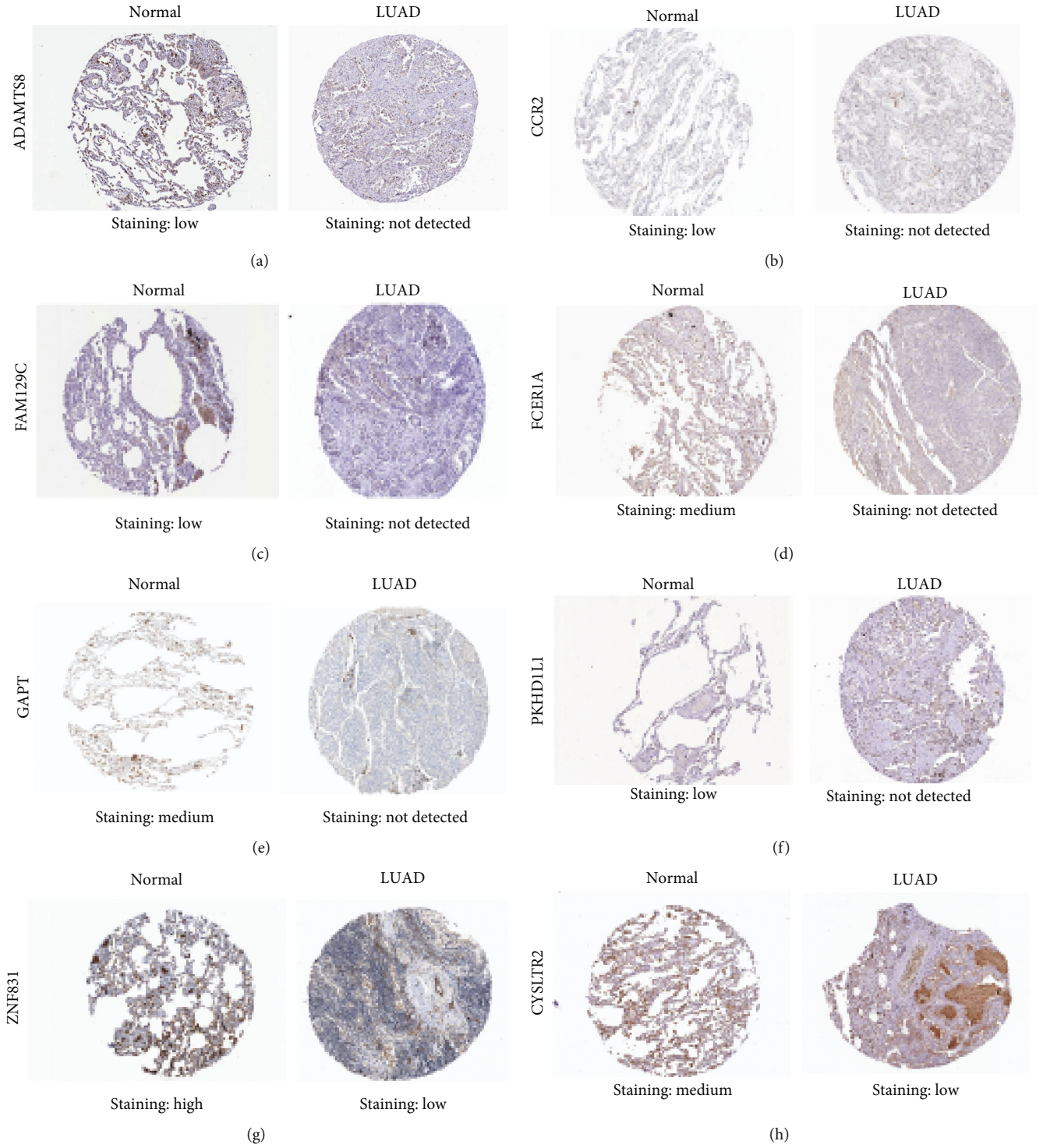

Figure 7: Relative immunohistochemistry results of 8 prognostic genes in LUAD tissues and normal lung tissues form the Human Protein Atlas database. The protein expression levels of 8 prognosis-related DEGs in LUAD and normal lung tissues by IHC images.

antibodies against the PD-1/PD-L1, has greatly improved cancer treatment and outcomes [22], especially for NSCLC [23]. Various studies have revealed the TME of NSCLC consists of various immune cells, indicating the prognostic value of TME immune cells [24]. In this study, we determined whether ESTIMATE scores of TME are indicative of overall survival and investigated the prognostic value of stromal and immune infiltration scores in LUAD. These scores predict patient clinical outcomes. Higher immune scores were associated with better LUAD prognosis, consistent with previous findings [25–27]. Tumors with high immune cell infiltrations in the TME exhibit favorable prognosis [28]. Our data

indicates that immune scores reflect survival and clinical outcomes in LUAD. It should be determined whether ESTIMATE immune scores are potential prognostic biomarkers.

The prognostic potential of stromal and immune scores has been determined for multiple cancers [29, 30]. Immune and stromal cells are the most important nontumor components in tumor tissues. Lung tissues contain infiltrating immune cells from innate and acquired immune components. The type, concentration, and localization of these immune factors may indicate prognostic outcomes for cancers and other pathologies. Tumor cells and other TME constituents secrete chemokines and chemokine receptors [31], which modulate the proliferation and invasion of malignant cells. The association between immune scores obtained by ESTIMATE analysis and disease prognosis across cancer types has been determined. Higher scores indicate better prognosis for breast cancer, melanoma, and ovarian cancer but poor prognosis for hepatocellular carcinoma [30]. The lung cancer TME is rich in immune cells [32]. In LUAD, high immune scores and high infiltrations by adaptive immune cells are associated with favorable outcomes.

FPR2 is a G protein coupled receptor (GPCR) that plays an important role in antibacterial inflammation. Upregulated FPR2 suppresses epithelial-mesenchymal transition of lung cancer cells [33]. Interestingly, certain genotypes of interleukins can predict the risk of death and progression, in NSCLC patients [34]. However, the mechanisms through which interleukins influence prognosis in NSCLC have not been established. We established that CCR2 is a hub and prognostic gene. CCR2 recruits precursors for exudative macrophages and inflammatory DCs into the lung. Until recently, biological functions of CCR2 in lung cancer had yet to be established. CCR2 induces macrophage and cancer cell crosstalk, an essential mechanism for driving lung cancer progression [35]. CCR2 is involved in promotion of tumor-supportive immune microenvironment [36]. In this study, elevated CCR2 levels correlated with longer survival time, consistent with previous findings [37]. Therefore, the role of CCR2 in lung cancer requires further investigations.

Although our study explored the prognostic genes based on TME of LUAD, their prognostic significance as well as the involved mechanisms were not determined. Moreover, our findings are based on bioinformatics analyses, and further validation should be performed in future studies.

This study elucidates on the prognostic potential of TME in LUAD and provides the foundation for further studies on prognostic biomarkers in LUAD.

Data Availability

The data used to support the findings of this study are available from the corresponding authors upon request. All data used in this study can be downloaded from TCGA (https://portal.gdc.cancer.gov/), GEO (https://www.ncbi.nlm.nih.gov/geo/), CPTAC (https://proteomics.cancer.gov/programs/cptac), and HPA (https://www.proteinatlas.org) databases.

Ethical Approval

There were no cell, tissue, or animal studies. No ethical requirements are involved.

Conflicts of Interest

The authors declare that there are no competing interests associated with the manuscript.

Authors' Contributions

QL and JZ are responsible for the integrity of this work. PH and YF conducted the statistical and bioinformatic analyses and prepared all figures and tables. QL, JZ, PH, and YF conceived and designed this study and wrote the manuscript. All authors have read and approved the final version of the manuscript. Pengkai Han and Yunxiu Fan contributed to this work equally.

Acknowledgments

We sincerely acknowledge researchers who constructed the public databases: TCGA, GEO, CPTAC, and HPA. The present study was funded by the Natural Science Foundation of Chongqing (cstc2020jcyj317msxmX1037) and Medical Science and Health Care Joint Medical Research Project of Wanzhou District, Chongqing (wzstc-kw202101), China.

Supplementary Materials

Supplementary 1. Figure S1: whole procedure for analyzing prognostic genes and immune landscape signatures based on tumor microenvironment in lung adenocarcinoma.

Supplementary 2. Table S1: marker genes for 29 immune cell subtypes.

Supplementary 3. Table S2: clinical characteristics of LUAD patients from TCGA and GEO cohorts.

Supplementary 4. Table S3: DEGs with significant correlation with overall survival of LUAD.

Supplementary 5. Table S4: DEGs with significant correlation with overall survival of LUAD data from GEO.

References

[1] A. L. Potter, A. L. Rosenstein, M. V. Kiang et al., "Association of computed tomography screening with lung cancer stage shift and survival in the United States: quasi-experimental study," *BMJ*, vol. 376, article e069008, 2022.

[2] M. Duruisseaux and M. Esteller, "Lung cancer epigenetics: from knowledge to applications," *Seminars in Cancer Biology*, vol. 51, pp. 116–128, 2018.

[3] D. Chakravarty and D. B. Solit, "Clinical cancer genomic profiling," *Nature Reviews Genetics*, vol. 22, no. 8, pp. 483–501, 2021.

[4] X. Jing, F. Yang, C. Shao et al., "Role of hypoxia in cancer therapy by regulating the tumor microenvironment," *Molecular Cancer*, vol. 18, no. 1, p. 157, 2019.

[5] T. Lan, M. Luo, and X. Wei, "Mesenchymal stem/stromal cells in cancer therapy," *Journal of Hematology & Oncology*, vol. 14, no. 1, p. 195, 2021.

[6] K. Khalaf, D. Hana, J. T. Chou, C. Singh, A. Mackiewicz, and M. Kaczmarek, "Aspects of the tumor microenvironment involved in immune resistance and drug resistance," *Frontiers in Immunology*, vol. 12, article 656364, 2021.

[7] B. M. Ku, Y. Kim, K. Y. Lee et al., "Tumor infiltrated immune cell types support distinct immune checkpoint inhibitor outcomes in patients with advanced non-small cell lung cancer," *European Journal of Immunology*, vol. 51, no. 4, pp. 956–964, 2021.

[8] A. Bagaev, N. Kotlov, K. Nomie et al., "Conserved pan-cancer microenvironment subtypes predict response to immunotherapy," *Cancer Cell*, vol. 39, no. 6, pp. 845–865.e7, 2021.

[9] S. Cao, C. Lin, X. Li, Y. Liang, and P. E. Saw, "TME-responsive multistage nanoplatform for siRNA delivery and effective cancer therapy," *International Journal of Nanomedicine*, vol. 16, no. 16, pp. 5909–5921, 2021.

[10] K. Yoshihara, M. Shahmoradgoli, E. Martínez et al., "Inferring tumour purity and stromal and immune cell admixture from expression data," *Nature Communications*, vol. 4, no. 1, p. 2612, 2013.

[11] W. T. Wu, Y. J. Li, A. Z. Feng et al., "Data mining in clinical big data: the frequently used databases, steps, and methodological models," *Military Medical Research*, vol. 8, no. 1, p. 44, 2021.

[12] H. Feng, Y. Zhao, W. Yan et al., "Identification of signature genes and characterizations of tumor immune microenvironment and tumor purity in lung adenocarcinoma based on machine learning," *Frontiers in Medicine*, vol. 9, no. 9, article 843749, 2022.

[13] P. Gaudet, C. Logie, R. C. Lovering, M. Kuiper, A. Lægreid, and P. D. Thomas, "Gene ontology representation for transcription factor functions," *Biochimica et Biophysica Acta (BBA) - Gene Regulatory Mechanisms*, vol. 1864, no. 11-12, article 194752, 2021.

[14] M. Kanehisa, Y. Sato, and M. Kawashima, "KEGG mapping tools for uncovering hidden features in biological data," *Protein Science*, vol. 31, no. 1, pp. 47–53, 2022.

[15] T. Wu, E. Hu, S. Xu et al., "clusterProfiler 4.0: A universal enrichment tool for interpreting omics data," *Innovations*, vol. 2, no. 3, article 100141, 2021.

[16] W. Lin, Y. Chen, B. Wu, Y. Chen, and Z. Li, "Identification of the pyroptosis-related prognostic gene signature and the associated regulation axis in lung adenocarcinoma," *Cell Death Discovery*, vol. 7, no. 1, 2021.

[17] S. Garinet, P. Wang, A. Mansuet-Lupo, L. Fournel, M. Wislez, and H. Blons, "Updated prognostic factors in localized NSCLC," *Cancers*, vol. 14, no. 6, p. 1400, 2022.

[18] L. Zhang, J. R. Conejo-Garcia, D. Katsaros et al., "Intratumoral T cells, recurrence, and survival in epithelial ovarian cancer," *The New England Journal of Medicine*, vol. 348, no. 3, pp. 203–213, 2003.

[19] W. Zhuang, H. Sun, S. Zhang et al., "An immunogenomic signature for molecular classification in hepatocellular carcinoma," *Molecular Therapy–Nucleic Acids*, vol. 25, pp. 105–115, 2021.

[20] C. L. Zheng, Q. Lu, N. Zhang et al., "Comprehensive analysis of the immune and prognostic implication of MMP14 in lung cancer," *Disease Markers*, vol. 2021, Article ID 5917506, 2021.

[21] W. Zhang, N. Borcherding, and R. Kolb, "IL-1 signaling in tumor microenvironment," *Advances in Experimental Medicine and Biology*, vol. 1240, pp. 1–23, 2020.

[22] T. Donnem, T. K. Kilvaer, S. Andersen et al., "Strategies for clinical implementation of TNM-Immunoscore in resected nonsmall-cell lung cancer," *Annals of Oncology*, vol. 27, no. 2, pp. 225–232, 2016.

[23] L. Horn, A. S. Mansfield, A. Szczęsna et al., "First-line atezolizumab plus chemotherapy in extensive-stage small-cell lung cancer," *The New England Journal of Medicine*, vol. 379, no. 23, pp. 2220–2229, 2018.

[24] P. Diao, Y. Jiang, Y. Li et al., "Immune landscape and subtypes in primary resectable oral squamous cell carcinoma: prognostic significance and predictive of therapeutic response," *Journal for Immunotherapy of Cancer*, vol. 9, no. 6, article e002434, 2021.

[25] J. Kargl, S. E. Busch, G. H. Y. Yang et al., "Neutrophils dominate the immune cell composition in non-small cell lung cancer," *Nature Communications*, vol. 8, no. 1, article 14381, 2017.

[26] Å. K. Öjlert, A. R. Halvorsen, D. Nebdal et al., "The immune microenvironment in non-small cell lung cancer is predictive of prognosis after surgery," *Molecular Oncology*, vol. 13, no. 5, pp. 1166–1179, 2019.

[27] M. Usó, E. Jantus-Lewintre, S. Calabuig-Fariñas et al., "Analysis of the prognostic role of an immune checkpoint score in resected non-small cell lung cancer patients," *Oncoimmunology*, vol. 6, no. 1, article e1260214, 2017.

[28] K. B. Givechian, C. Garner, S. Benz, B. Song, S. Rabizadeh, and P. Soon-Shiong, "An immunogenic NSCLC microenvironment is associated with favorable survival in lung adenocarcinoma," *Oncotarget*, vol. 10, no. 19, pp. 1840–1849, 2019.

[29] X. Zhu, X. Xie, Q. Zhao, L. Zhang, C. Li, and D. Zhao, "Potential prognostic value and mechanism of stromal-immune signature in tumor microenvironment for stomach adenocarcinoma," *BioMed Research International*, vol. 2020, Article ID 4673153, 15 pages, 2020.

[30] H. Wang, J. Rong, Q. Zhao et al., "Identification and validation of immune cells and hub genes in gastric cancer microenvironment," *Disease Markers*, vol. 2022, no. 5, Article ID 8639323, 2022.

[31] D. C. Hinshaw and L. A. Shevde, "The tumor microenvironment innately modulates cancer progression," *Cancer Research*, vol. 79, no. 18, pp. 4557–4566, 2019.

[32] H. Peng, X. Wu, R. Zhong et al., "Profiling tumor immune microenvironment of non-small cell lung cancer using multiplex immunofluorescence," *Frontiers in Immunology*, vol. 12, article 750046, 2021.

[33] Q. Wang, B. Hu, X. Hu et al., "Tumor evolution of glioma-intrinsic gene expression subtypes associates with immunological changes in the microenvironment," *Cancer Cell*, vol. 32, no. 1, pp. 42–56.e6, 2017.

[34] H. J. Lee, M. K. Park, E. J. Lee, and C. H. Lee, "Resolvin D1 inhibits TGF-β1-induced epithelial mesenchymal transition of A549 lung cancer cells via lipoxin A4 receptor/formyl peptide receptor 2 and GPR32," *The International Journal of Biochemistry & Cell Biology*, vol. 45, no. 12, pp. 2801–2807, 2013.

[35] C. Pérez-Ramírez, M. Cañadas-Garre, A. Alnatsha et al., "Interleukins as new prognostic genetic biomarkers in non-small cell lung cancer," *Surgical Oncology*, vol. 26, no. 3, pp. 278–285, 2017.

[36] A. Schmall, H. M. Al-tamari, S. Herold et al., "Macrophage and cancer cell cross-talk via CCR2 and CX3CR1 is a fundamental mechanism driving lung cancer," *American Journal of Respiratory and Critical Care Medicine*, vol. 191, pp. 437–447, 2015.

[37] T. Hartwig, A. Montinaro, S. von Karstedt et al., "The TRAIL-induced cancer secretome promotes a tumor-supportive immune microenvironment via CCR2," *Molecular Cell*, vol. 65, no. 4, pp. 730–742.e5, 2017.